

# The spatial inhomogeneity of pressure inside a violin at main air resonance

Guy Vandegrift

*Department of Physics, The University of Texas at El Paso, El Paso, Texas 79968-0515*

Eccles Wall

*Greensboro College, Greensboro, North Carolina 27412*

(Received 8 February 1996; revised 15 November 1996; accepted 27 March 1997)

The fluctuating pressure inside a violin is investigated at the  $A0$  (main air) resonance, under the assumption that the walls are kept rigid. Three effects are shown to contribute to a reduction in the fluctuating pressure near the violin's  $f$ -holes. The strongest effect arises from a tendency to form a standing wave within the relatively long, thin shape of the upper bout. A second and smaller effect arises from the violin's nonuniform shape, and is modeled by treating the upper bout as an acoustical waveguide with nonuniform cross section. A third effect is associated with the Green's function of an acoustical radiator, and will significantly reduce the fluctuating pressure in the immediate vicinity of the violin's  $f$ -hole. Experimental verification of the theory is obtained by measuring the fluctuating pressure inside a rectangular box, with the resonance being driven by a small loudspeaker located outside the aperture. © 1997 Acoustical Society of America. [S0001-4966(97)06107-9]

PACS numbers: 43.75.De [WJS]

## INTRODUCTION

The violin's main air resonance ( $A0$  mode) strongly resembles a Helmholtz resonator, which is characterized by a small aperture and uniform fluctuating pressure throughout the chamber.<sup>1-5</sup> However, the upper bout of the violin is sufficiently long and thin, and the  $f$ -hole sufficiently large, that the  $A0$  mode also somewhat resembles the quarter wavelength mode of an open-ended resonator.<sup>2,3,6,7</sup> Other complications are:

- (1) the violin's nonuniform shape;<sup>6-9</sup>
- (2) the aperture acting as an acoustical radiator;<sup>10,11</sup>
- (3) the flexibility of the walls (i.e., coupling to wood modes).<sup>5</sup>

This paper investigates the inhomogeneity in fluctuating pressure inside the violin at the  $A0$  mode, under the simplifying assumption that the walls are rigid. However, the conclusions are relevant to the fact that the plates of a violin do flex. Cremer<sup>5</sup> describes a linear model that treats the violin as two or more rigid plates held by spring mechanisms. The air near an  $f$ -hole is treated simply as another mass with an associated spring constant caused by the compressibility of air.<sup>4</sup> The equations in this model resemble those of a discrete set of masses linked by harmonic springs. In its simplest version, only two masses are considered: one wall that moves as a piston, and one mass of air localized to a region near the  $f$ -hole. This yields two modes: the air ( $A0$ ) mode, and a "wood" mode, taken to represent the  $T1$  mode,<sup>12-15</sup> higher in frequency by a factor of approximately 1.5. Coupling between air and wood motion is shown<sup>5</sup> to lower the frequency of the air mode  $\omega_0$  to a value perhaps 5%–7% lower than the classical Helmholtz frequency  $\omega_H$  [i.e.,  $\omega_H \approx c(L_f/V_T)^{1/2}$ , where  $c$  is the speed of sound,  $V_T$  is the total

volume of the violin, and  $L_f$  is the sum of the lengths of the two  $f$ -holes<sup>4</sup>].

Measurements of the violin's bridge admittance,  $|v(\omega)/F(\omega)|$ , exhibit several dips and peaks as the frequency  $\omega$  is varied.<sup>5,14,15</sup> Cramer's simple two-mass model suggests an explanation for this as it predicts a bridge admittance which diverges at  $\omega = \omega_O$  and vanishes at  $\omega = \omega_H$ . (Note that  $\omega_O$  is the resonant frequency of the air mode after it has been shifted away from the "Helmholtz" frequency  $\omega_H$  by wood-coupling effects. For the sake of simplicity, the two-mass model justifiably neglects any frequency shifts due to complications in air motion described later in this paper.)

Cremer refers to the region on the upper plate between the  $f$ -holes as the "island," and argues that it plays an important role in the coupling of air and wood motion. This coupling depends on the mass and stiffness of the wood, as well as on the fluctuating air pressure, especially at locations of maximum plate motion. Holographic studies of the violin's motion at the  $T1$  mode indicate that motion is indeed large near the  $f$ -holes, although not so large that the relatively small "island" completely dominates the production of sound.<sup>5</sup> In a demonstration not recommended on a good violin, one can see the wood flex and hear a change in tone by pressing hard on the instrument near the  $f$ -hole. While this change in tone may be due to changes in harmonics higher than the frequencies of interest, it suggests that the magnitude of fluctuating air pressure at the  $f$ -holes might be important. While not all investigations of pressure inside the violin at the  $A0$  resonance have reported a reduction of pressure near the  $f$ -holes, our analysis clearly predicts that such a reduction should exist.<sup>8,15</sup>

A completely uniform fluctuating pressure is associated with an ideal Helmholtz resonator and occurs if the  $f$ -hole is sufficiently small. This can be understood as follows: If the size of the cavity,  $L$ , is kept constant, then a reduction in

aperture size reduces the resonance frequency  $\omega = k/c$  to the pint where  $kL \ll 1$ , so that a sound wave would transit the cavity in a time much less than a period of oscillation. Thus the air comes to a sort of mechanical equilibrium with respect to sound vibrations at very low frequencies. Shaw<sup>8</sup> has modeled the A0 mode using acoustical impedances and concluded from both calculations and measurements that the pressure in the upper bout is 30%–40% higher than in the lower bout. This is due to inductances (kinetic energy of air) not associated with the f-holes. In a classical Helmholtz resonator, all the acoustical inductance is at the aperture, while the cavity provides all the acoustical capacitance (potential energy of compression). We have analyzed the acoustical circuit of Fig. 2(c) in Shaw's paper, taking the limit that the inductance  $L_f$  goes to infinity, which corresponds to a vanishingly small f-hole. As one would expect, the fluctuating pressures in the upper and lower bout are equal in this limit.

Standing waves in an acoustical waveguide arise from capacitance and inductance distributed equally along the waveguide. As the frequency of the mode is increased (by increasing aperture area), there is a tendency to form a standing wave inside the violin. We shall call this tendency the "standing-wave" effect, and it causes the fluctuating pressure to increase slightly as one moves away from the aperture. The distance from the middle of an f-hole to the top of the upper bout is about 18 cm, while a quarter wavelength for the main air resonance (A0 at 285 Hz) is 30 cm. The lower part of the violin is about 15 cm long, so that a smaller standing-wave effect would be expected in the lower bout. A highly simplistic model of the pressure difference between the upper and lower bouts is obtained by modeling two standing waves with pressures that match at the f-holes. Using the wavelengths and lengths listed above, one can obtain a crude estimate of the difference in pressure between the upper and lower bout by taking the pressure to be sinusoidal and assuming antinodes ( $\partial p / \partial z = 0$ ) at the top and bottom. This simple estimate yields a 20% difference between the pressure at the top of the upper bout and the bottom of the lower bout. In this article, we shall focus on the upper bout because it should exhibit the stronger inhomogeneity in pressure fluctuations. However, the methods discussed can be applied to the lower bout as well.

Aside from the "standing-wave" effect, one must consider two other effects. The "shape" effect is due to the constriction near the center of the violin, apparently designed to allow room for the bow. It produces a discontinuous change in the slope of the pressure whenever the cross-sectional area changes abruptly, as shown schematically in Fig. 1. In the case of a violin, the "shape" effect enhances the "standing-wave" effect, although only slightly, as we shall see later. The "source" effect arises from the Green's function for an acoustical radiator inside a cavity.<sup>10,11</sup> It also causes a drop in pressure near the aperture, as sketched in Fig. 1. In contrast to the "shape" effect, which occurs only when the chamber is long and thin, the "source" effect is present in every Helmholtz resonator, provided one is sufficiently close to the aperture.

Our analysis indicates that the "standing-wave" effect is the dominant non-Helmholtz effect throughout the upper

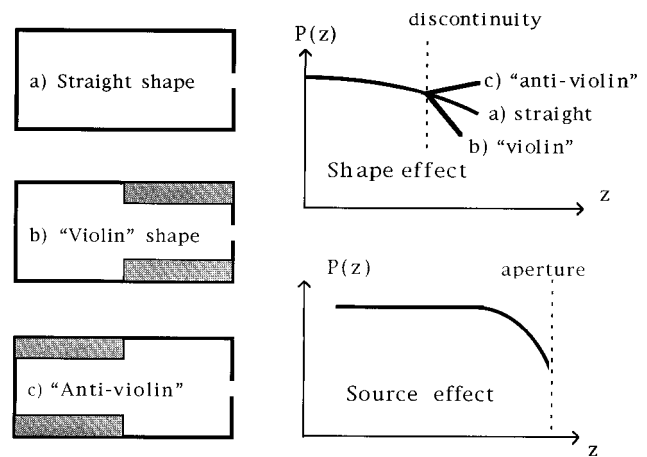


FIG. 1. The fluctuating pressure inside a rectangular cavity with irregular cross section depends on whether the shape is (a) "straight," (b) "violin-like," or (c) opposite that of the violin, i.e., "antiviolin." The "shape effect" is shown for a discontinuity in the cross-sectional area of the chamber. The "source" effect is a sudden drop in pressure near the aperture.

bout of the violin. However, both the "shape" and "source" effects should exert a small influence throughout most of the upper bout. And, we predict that the "source" effect will significantly reduce the fluctuating pressure at close proximity to the f-hole.

## I. THEORY

The source effect arises from the fact that the aperture radiates with phase opposite to the uniform pressure fluctuation associated with the Helmholtz resonance.<sup>10,11</sup> We start by integrating the Green's function over the surface of the aperture, noting that the first and larger term yields a constant, independent of position, which we denote as  $P_1$ :

$$p(\mathbf{r}) = \int \int \left\{ \frac{1}{k^2 V} - \frac{1}{4\pi} \frac{N}{|\mathbf{r} - \mathbf{r}'|} \right\} \sigma(\mathbf{r}') d^2 \mathbf{r}'$$

$$\approx \left[ 1 - \frac{Nk^2 V}{4\pi} \left\langle \frac{1}{s} \right\rangle \right] P_1, \quad (1)$$

where  $\sigma = -j\omega(\mathbf{v} \cdot \mathbf{n})$  is proportional to the velocity fluctuation at the aperture, with the convention  $\partial/\partial t = j\omega$ . We denote  $\langle 1/s \rangle$  to be the weighted average of the inverse of the distance  $|\mathbf{r} - \mathbf{r}'|$  from the field point  $\mathbf{r}$  to source points  $\mathbf{r}'$  on the aperture.  $N$  is associated with image sources and depends on the location of the aperture:

- $N=2$  if near center of a wall;
- $N=4$  if at a corner between two walls;
- $N=8$  if at a corner between three walls.

The source effect appears to be unrelated to the Bernoulli principle ( $2\delta P = -\rho \delta v^2$ ), which is nonlinear and therefore negligible at low amplitude. A physical appreciation of the source effect is obtained by considering a double Helmholtz resonator, formed by joining two identical resonators at the aperture. Since the two pressures in each chamber are out of phase, the aperture is an antinode in velocity and a node in pressure. In the case of a single resonator, we shall see that the fluctuating pressure at the aperture is reduced, but typically not to zero.

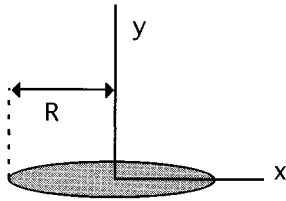


FIG. 2. The geometry used to deduce the pressure near a circular aperture of radius  $R$ .

For distances much greater than the size of the aperture, one may take  $\langle 1/s \rangle$  to be the inverse distance to the center of the aperture. However, since the source effect is strong only near the aperture, it is best to find  $\langle 1/s \rangle$  by integrating over the surface of the aperture. For thin walls and a small circular aperture, this integration is equivalent to calculating the potential of a charged disk.<sup>1,5</sup> Define  $x$  and  $y$  so that the distance to the center of the aperture of radius  $R$  is  $s = (x^2 + y^2)^{1/2}$ , as shown in Fig. 2. From Ref. 16, one can deduce

$$\begin{aligned} \left\langle \frac{1}{s} \right\rangle &= \frac{1}{R} \arctan\left(\frac{R}{y}\right) \text{ if } x=0, \\ \left\langle \frac{1}{s} \right\rangle &= \frac{1}{R} \arcsin\left(\frac{R}{x}\right) \text{ if } y=0 \text{ and } x \geq R, \\ \left\langle \frac{1}{s} \right\rangle &= \frac{1}{R} \left\{ \frac{\pi}{2} \right\} \text{ if } y=0 \text{ and } x \leq R. \end{aligned} \quad (2)$$

The case  $y=0$  corresponds to a determination of pressure along a line in contact with the wall and entering the aperture at  $x \leq R$ . Using Eq. (1) and  $k = (2R/V)^{1/2}$  for a small circular aperture, one obtains  $\langle Nk^2 V/4\pi s \rangle = 1/2$  on the surface of the aperture. Thus the fluctuating pressure at the aperture is half that within the chamber, if the aperture is not at a corner. In the Appendix, this is shown to be a general result for an ‘‘ideal’’ Helmholtz resonator (i.e., a resonator in which the ‘‘shape’’ and ‘‘standing-wave’’ effects are absent).

Next, we consider the shape effect, which in contrast to the source effect, is well known in that it is related to the joining of two acoustical waveguides of different areas.<sup>2,3</sup> Here, we show that the shape effect can also be obtained using Webster’s horn equation<sup>2,3,17,18</sup> for a waveguide of nonuniform cross-sectional area  $A = A(z)$ :

$$k^2 p + \frac{1}{A} \frac{\partial}{\partial z} \left( A \frac{\partial p}{\partial z} \right) = 0, \quad (3)$$

where  $p(z)$  is the fluctuating pressure. The boundary conditions are that  $\partial p/\partial z$  vanishes at the end opposite the aperture, and that both  $p$  and  $A \partial p/\partial z$  be continuous, the latter being proportional to the air flux ( $\rho \partial v/\partial t = -\partial p/\partial z$ ). The boundary conditions are sufficient, provided  $\omega$  is known. Let  $z$  be the distance to the end opposite the aperture, and let  $z = a$  be the point where the area changes by a factor  $1/\beta$ . (For example,  $A = 1$  for  $z < a$  and  $A = 1/\beta$  for  $z/a$ .) For  $z < a$ , we have

$$p(z) = P \cos(kz) \cos(\omega t), \quad (4)$$

and, for  $z > a$ ,

$$p(z) = P [C_1 \cos(kz) + C_2 \sin(kz)] \cos(\omega t). \quad (5)$$

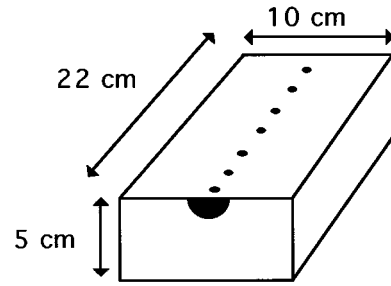


FIG. 3. A sketch of the resonant cavity. The shaded area is the aperture, and the line of black holes are plugged access holes for the microphone.

Using the continuity of  $p(z)$  and  $A \partial p/\partial z$  at  $z = a$  yields

$$\begin{aligned} C_1 &= \cos^2(ka) + \beta \sin^2(ka), \\ C_2 &= (1 - \beta) \cos(ka) \sin(ka). \end{aligned} \quad (6)$$

A conventional analysis of the ‘‘shape’’ effect, obtained by joining acoustical waveguides of different area, yields the same result.<sup>2,3</sup>

Since the ‘‘shape’’ and ‘‘source’’ effects tend to be located at different locations, we shall combine them in an *ad hoc* fashion by multiplying Eqs. (4) and (5) by the factor in front of  $P_1$  in Eq. (1).

## II. EXPERIMENT

In order to eliminate complications caused by the exotic shape and plate flexibility associated with a real violin, we designed an experimental resonator that was not a simulation of a violin, but rather an effort to establish the correctness of our theory. Since the shape effect is small for an actual violin, we designed our resonant cavity in order to exaggerate this effect. The rectangular cavity shape allowed us to introduce large discontinuities in cross section by inserting blocks into the chamber.

The air resonance was driven by a small speaker placed approximately 1 cm from the aperture, as was previously done in an investigation of the main air resonance of a violin.<sup>4</sup> The resonant cavity was a plywood box of dimensions 22×5×10 cm, with seven plugged holes located along the center of one wall, as shown in Fig. 3. The fluctuating pressure was measured at each plugged hole by replacing the plug by a small microphone<sup>19</sup> that fit into the hole flush with the inner wall of the box. A semicircular aperture of radius 1.5 cm was cut from an aluminum plate that formed the front face of the box. The aluminum plate was clamped to the box, and ‘‘plastic wood’’ was used at the holes so that the microphone and plugs would fit snugly. Two wooden blocks of length 11.4 cm were inserted into the chamber to reduce the cross-sectional area of the chamber by a factor of 0.424. In this manner, all three cavity shapes shown in Fig. 1 could be studied. The resonant frequencies for the ‘‘straight,’’ ‘‘violin,’’ and ‘‘anti-violin’’ shapes are 173, 172, and 210 Hz, respectively.

Since this aperture is at a corner between two walls, three image sources will also contribute to the Green’s function, so that  $N=4$  in Eq. (1). On the other hand, we can model the semicircular aperture as a full circle by pretending

the cavity had twice the volume  $V$ , with the aperture being located at the center of a wall ( $N=2$ ). Since  $N$  and  $V$  enter as a product in Eq. (1), we see that both treatments yield identical values for magnitude of the source effect. The inverse distance  $\langle 1/s \rangle$  is the same for both geometries, provided we always average over the source and all its images.

Figure 4 displays the experimentally measured pressure as well as theoretical curves showing the relative importance of the “shape” and “source” effects. The seven experimental data points exhibit both an apparent change in slope of pressure (shape effect) and a significant drop in pressure near the aperture (source effect). The solid line shows our theoretical prediction for each of the three shapes. In order to deduce the relative importance of the three effects, we have used dashed lines to plot versions of the theory that do not include certain effects. The dashed line for the straight shape is a simple model which takes the pressure variation to be  $\cos(kz)$ , thus incorporating only the “standing-wave” effect. The full model, incorporating all the effects, appears to give the best fit to the experimental data for all three shapes.

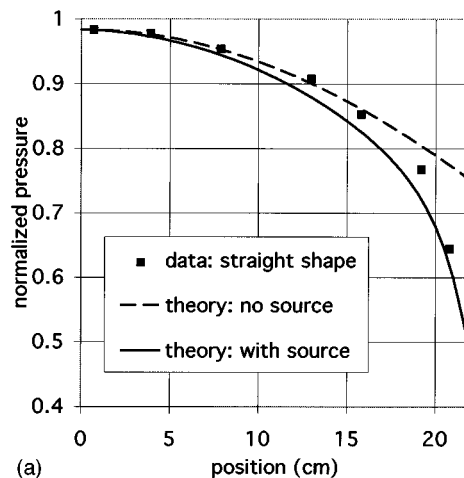
The curves in Fig. 4 do not show the pressure falling to the value  $(1/2)P$ , as discussed in the Appendix and following Eq. (2). This occurs because our resonator is not an ideal Helmholtz resonator, which is characterized by incompressible airflow confined to the region very close to a small aperture.

### III. APPLICATION TO A VIOLIN

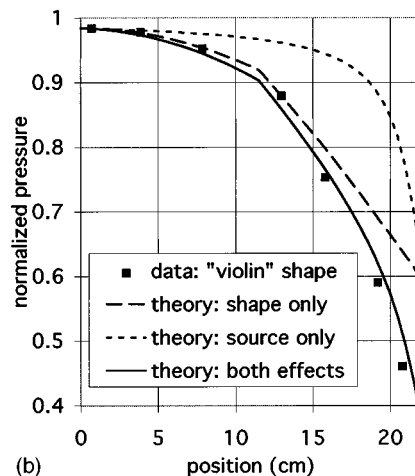
We shall now apply these ideas to the upper bout of an actual violin. For our calculation, we divide the chamber into four parts and consider one-fourth of a violin with half an f-hole. Picture the violin with the f-holes facing you and the fingerboard at the top. Bisect the violin with a vertical line along the corpus centerline. Then cut the violin into two pieces, top and bottom, near the center of the f-holes, so that we are left with a single cavity with an aperture that consists of half of one f-hole, located at the corner between two walls. The following parameters are used:  $L=18$  cm,  $\beta=1.2$ , and  $V=600$  cm<sup>3</sup> (one-fourth the actual volume). The discontinuity in area is taken to be 11 cm from the top of the upper bout.

A crude model of the f-hole is obtained by treating one f-hole as two closely spaced circles or radius 0.8 cm, centered 3.2 cm apart, with one hole being within our subdivided chamber, centered at  $z_A=16.4$  cm. An estimate of frequency, using a circular aperture, yields  $2\pi f \approx c(2R/V)^{1/2}=282$  Hz.<sup>1-3</sup> A compromise must be made between matching to the area of a typical f-hole (4–6 cm<sup>2</sup>) or to the A0 frequency (275–295 Hz). Fortunately, the calculated pressure is not strongly sensitive to variations in these parameters. This insensitivity also suggests that we are justified in using a simple estimate of resonant frequency that neglects both shape effects and aperture images.

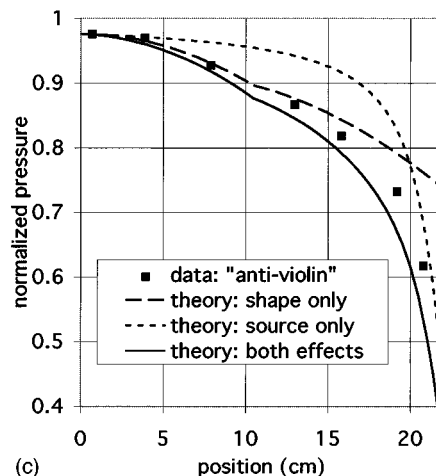
The solid line of Fig. 5 (labeled “along to plate”) shows the prediction for points located on the top plate for a path starting from the uppermost region of the upper bout leading to contact with an aperture. Since the airflow resembles the electric field on a charged conducting disk, the fluctuating pressure should be uniform at the aperture, as shown in the



(a)



(b)



(c)

FIG. 4. Experimental data for the three configurations: (a) straight, (b) violin, (c) anti-violin. Squares show experimentally observed data. The solid lines are theoretical predictions which include all effects. The dashed lines show theoretical predictions when only the source or only the shape effects are included. The dashed line for the straight shape is a simple model which takes the pressure variation to be  $\cos(kz)$ .

figure. In order to make a graph with this uniform pressure, we have suppressed the variation associated with shape effects at the f-hole. In other words, for values of  $z$  located beyond the f-hole at  $z_A$ , Eq. (1) is multiplied by an appropriate constant instead of by Eq. (5). This difficulty in ob-

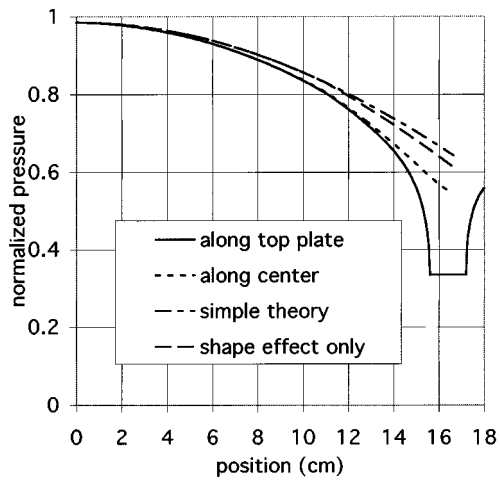


FIG. 5. A theoretical curve showing the pressure inside a violin. The solid line (along top plate) shows the prediction for points located on the top plate on a path starting from the uppermost region of the upper bout leading to contact with an f-hole, with the shape effect being suppressed only at the aperture. The three dashed lines calculate the pressure along a path located 2 cm below the top plate. The curve “along center” incorporates the full theory, incorporating both shape and source effects. “Simple theory” neglects both shape and source effects by assuming  $pc \cos(kz)$ . “Shape effect only” includes the shape effect, but neglects the source effect.

taining a uniform pressure at the surface of the aperture suggests that the *ad hoc* method of multiplying both effects may not be valid when both “source” and “standing-wave” effects are large.

The three dashed lines in Fig. 5 show calculated pressure at points 2 cm below the top plate, taking  $\langle 1/s \rangle^{-1}$  to be  $((z - z_A)^2 + 2^2)^{1/2}$ . In order to establish the relative importance of the various effects, predictions of the full theory, as well as simplified versions are shown. The line marked “along center” represents our best estimate, incorporating the full theory including both shape and source effects. The curve labeled “simple theory” neglects both shape and source effects by assuming a pressure proportional to  $\cos(kz)$ . This “simple” theory models only the “standing-wave” effect, and is adequate for most of the upper bout, but fails somewhat near the f-holes. The curve marked “shape effect only” includes the shape effect, but neglects the source effect. This curve is almost identical to the “simple theory,” which suggests that the shape effect is relatively unimportant in modeling the pressure variation in a violin.

In conclusion, the fluctuating pressure inside a Helmholtz resonator is nonuniform for two reasons: First, the aperture acts as an acoustical source, causing the pressure to drop in the immediate vicinity of the aperture. Second, if the resonator is long and thin, there is a tendency to form a standing wave in the cavity, with the high pressure being located in the back of the chamber. This effect is enhanced if the chamber has a discontinuity in the cross-sectional area of the form found in the violin’s upper bout. Both theoretical and experimental evidence indicates that the fluctuating pressure inside a violin is considerably lower near the f-holes than would be predicted by simply modeling the main air resonance as a classical Helmholtz resonator.

## ACKNOWLEDGMENT

The authors are grateful to the University of North Carolina, Greensboro for the use of equipment and the purchase of the microphone.

## APPENDIX: DERIVATION OF $\langle Nk^2V/4\pi s \rangle = 1/2$ AT THE APERTURE FOR AN IDEAL HELMHOLTZ RESONATOR WITH $N=2$

Here, we show that for an ideal Helmholtz resonator, the fluctuating pressure at the aperture is exactly one-half of the fluctuating pressure throughout the rest of the chamber, provided that the aperture is not at a corner. In keeping with this assumption of an ideal Helmholtz resonator, we take the fluctuating pressure to have the uniform value  $P_1$  throughout most of the chamber. Thus we assume a very small aperture, and, consequently, a low value of  $k = \omega/c$ , so that the “shape” and “standing-wave” effects are absent.

The simplest proof is based on the null in fluctuating pressure at the aperture for the double Helmholtz resonator described in Sec. I. One notes that, if an identical resonator is placed on the other side of the aperture, then symmetry dictates a pressure node at the aperture. Hence the factor  $\langle Nk^2V/4\pi s \rangle$  in Eq. (1) must be unity for a double resonator. Next, we observe that the factor  $\langle 1/s \rangle$  in Eq. (1) is independent of whether the resonator is single or double. However,  $k = \omega/c$  decreases by a factor of  $2^{1/2}$  for a single resonator because the “mass” of the air remains the same when the “spring constant”<sup>4</sup> is halved in the process of converting a double resonator into a single one. Hence,  $\langle Nk^2V/4\pi s \rangle$  is half as big for a single Helmholtz resonator as it is for a double resonator. Therefore,  $\langle Nk^2/4\pi s V \rangle = 1/2$  on the surface of a single Helmholtz resonator.

A more detailed proof is based on an analog between air velocity and electrostatic field at low  $\omega$ .<sup>1</sup> The maximum kinetic energy  $T$  and the potential energy  $U$  of a Helmholtz resonator are

$$T = \frac{\rho_0}{2} \int v^2 d\tau, \quad U = \frac{c^2 \rho_0}{2V} \left[ \int \frac{\mathbf{v} \cdot d\mathbf{a}}{\omega} \right]^2,$$

where  $\rho_0$  is the mass density of air. [This formula for potential energy can be obtained from Eq. (2) of Ref. 4, with the substitution of  $\int \mathbf{v} \cdot d\mathbf{a}$  for  $\omega \xi (\pi R^2)$ , where  $\xi$  is the displacement of the cylinder of air and  $K$  is the spring constant. Note that  $U = (1/2)K\xi^2$  and  $c^2 = \gamma P_0 / \rho_0$ .] Setting  $T = U$  yields

$$k^2 V = \frac{[\int \mathbf{v} \cdot d\mathbf{a}]^2}{\int v^2 d\tau},$$

from which the resonant frequency of an ideal Helmholtz resonator can be deduced. Since the manipulations to follow are quite familiar in electrostatics, we use a notation that follows from viewing  $\mathbf{v} = -\nabla \Phi^*$  as an electric field, where  $\Phi^*$  is the analog to electrostatic potential at the aperture. Other analogs are  $E^*$ ,  $Q^*$ , and  $\rho^*$ , representing energy, charge, charge density, and potential, respectively. From any good textbook on electrostatics,<sup>16</sup> we have (in cgs units):

$$E^* = \frac{1}{8\pi} \int v^2 d\tau = \frac{1}{2} (Q^*)(\Phi^*),$$

$$\int v \cdot d\mathbf{a} = 2\pi Q^*,$$

$$\Phi^*(\mathbf{r}_A) = \int \frac{\rho^*}{|\mathbf{r}-\mathbf{r}'|} d\tau' \equiv Q^* \left\langle \frac{1}{s} \right\rangle,$$

provided  $\mathbf{r}$  is somewhere on the surface of the aperture. (In contrast to electrostatic calculations, the surface integral of velocity here is taken over only one surface.) Algebraic manipulation of these equations gives our results:

$$\frac{k^2 V}{2\pi} \left\langle \frac{1}{s} \right\rangle = \frac{1}{2}.$$

Lest there be any doubt, a third proof is offered. The fluctuating pressure far outside the resonator is zero because the radiation field is small, owing to the low frequency and small aperture size. The line integral of  $\mathbf{v}$  from far outside the resonator to deep inside is proportional to  $P_1$  because  $j\omega\rho\int\mathbf{v}\cdot d\mathbf{r}=P_1$  (recall that  $\rho\partial\mathbf{v}/\partial t=j\omega\mathbf{v}=-\nabla p$ ). If the aperture is not near a corner, the air flow pattern is identical inside and outside the resonator. Therefore, by symmetry, the line integral representing pressure starts at 0 far outside the resonator, reaches  $P_1/2$  at the aperture, and finally asymptotes to  $P_1$  deep within the ideal Helmholtz resonator.

<sup>1</sup>Lord Rayleigh, *The Theory of Sound* (Macmillan, London, 1929), Chap. XVI, Art. 303-307, pp. 170-83.

<sup>2</sup>A. D. Pierce, *Acoustics* (McGraw-Hill, New York, 1981), Chap. 7.

<sup>3</sup>L. E. Kinsler and A. R. Frey, *Fundamentals of Acoustics* (Wiley, New York, 1982), 3rd ed., Chap. 10.

<sup>4</sup>G. Vandegrift, "Experimental investigation of the Helmholtz resonance of a violin," *Am. J. Phys.* **61**, 415-421 (1993).

<sup>5</sup>L. Cremer, *The Physics of the Violin* (MIT, Cambridge, MA, 1984), Chaps. 10 and 13.

<sup>6</sup>B. Denardo and S. Alkov, "Acoustic resonators with variable nonuniformity," *Am. J. Phys.* **62**, 315-321 (1994).

<sup>7</sup>B. Denardo and M. Bernard, "Design and measurements of variably non-uniform acoustic resonators," *Am. J. Phys.* **64**, 745-751 (1996).

<sup>8</sup>E. A. Shaw, "Cavity resonance in the violin: Network representation and the effect of damped and undamped ribholes," *J. Acoust. Soc. Am.* **87**, 398-410 (1990).

<sup>9</sup>E. V. Jansson, "Acoustical properties of complex cavities. Prediction and measurements of resonance properties of violin-shaped and guitar-shaped cavities," *Acustica* **37**, 211-221 (1977).

<sup>10</sup>G. Vandegrift, "A simple derivation of the Gren's function for a rectangular Helmholtz resonator at low frequency," *J. Acoust. Soc. Am.* **94**, 574-575 (1993).

<sup>11</sup>J. Van Bladel, "Coupling through small apertures with an application to Helmholtz' resonator," *J. Acoust. Soc. Am.* **45**, 604-613 (1969).

<sup>12</sup>E. Jansson, I. Milin, and J. Meyer, "Investigations into the acoustical properties of the violin," *Acustica* **62**, 1-15 (1986).

<sup>13</sup>K. Marshal, "Modal analysis of a violin," *J. Acoust. Soc. Am.* **77**, 695-709 (1985).

<sup>14</sup>J. A. Moral and E. V. Jansson, "Eigenmodes, input admittance, and the function of the violin," *Acustica* **50**, 329-337 (1982).

<sup>15</sup>I. M. Firth, "Modal analysis of the air cavity of the violin," *J. Catgut Acoust. Soc.* **48**, 17-24 (1987).

<sup>16</sup>J. D. Jackson, *Classical Electrodynamics* (Wiley, New York, 1975), p. 92. [Note that Eq. 3.178 in this 1st edition is in error, and the entire calculation is absent from the 2nd edition.]

<sup>17</sup>E. Eisner, "Complete solutions of the Webster horn equation," *J. Acoust. Soc. Am.* **41**, 1126-1146 (1967).

<sup>18</sup>A. H. Benade, "The Physics of Brasses," *Sci. Am.* (July 1973). Reprinted in *The Physics Music* (Freeman, San Francisco, 1977).

<sup>19</sup>The microphone was a 0.75-cm-diam "Tie-Pin" microphone obtained from Radio Shack: Cat. No. 33-1063 (Cost ~\$30).